Results in Chemistry 8 (2024) 101580

Contents lists available at ScienceDirect

Results in Chemistry

journal homepage: www.sciencedirect.com/journal/results-in-chemistry

Analysis of non-linear optical properties of phytochemical photosensitizers in cancer photodynamic therapy by quantum computational

V.M. Aneesa [a], K.P. Safna Hussan [b,c,*], S. Lekshmi [d], Thekkekara D. Babu [b], K. Muraleedharan [e,*]

[a] Majlis Arts and Science College, Puramannur, Malappuram - 676 552, Kerala, India
[b] Department of Biochemistry, Amala Cancer Research Center, Thrissur - 680 555, Kerala, India
[c] Ayurgreen Scientifica Research Institute, Ayurgreen Campus, Kavilpadi, Kaladi, Malappuram - 679 582, Kerala, India
[d] Department of Physics, Sanatana Dharma College, Alapuzha - 688 003, Kerala, India
[e] Department of Chemistry, University of Calicut, 673 635, Kerala, India

ARTICLE INFO

Keywords:
Photodynamic therapy
Photosensitizers
Phytochemicals
Non-linear optical properties
Quantum computational calculations

ABSTRACT

Rationale: Photodynamic therapy (PDT) is based on the reactive oxygen species (ROS) generated by light-activated photosensitizers in the presence of oxygen. Phytochemicals are promising natural photosensitizers, offering a potentially less toxic alternative for cancer treatments. Nonlinear optics (NLO) phenomena, such as second-harmonic generation (SHG), third-harmonic generation (THG), and two-photon absorption (TPA), can enhance light interaction, benefiting photosensitizing applications in PDT. Analyzing the NLO properties of phytochemicals can optimize their use in PDT by improving photosensitizer performance and efficacy.
Aim: This study aims to examine the NLO properties of selected phytochemicals in a reported polyherbal formulation to understand their potential as effective photosensitizers in PDT, thereby advancing cancer treatment options.
Methods: Quantum computational calculations were conducted at the B3LYP/6311 G++(d,p) level of theory to unveil crucial information about structural geometry and nonlinear optical properties.
Results: The bandgap of aloe emodin, emodin, curcumin, scopoletin berberine, furanocoumarin, rubiadin are 3.279 eV, 3.395 eV, 3.247 eV, 3.930 eV, 2.878 eV, 4.463 eV and 3.546 eV, respectively. The results highlight berberine as the most reactive compound, demonstrating high softness and low hardness. Curcumin and furanocoumarin exhibit distinct electron-donating and accepting tendencies, respectively. In the MESP map of furanocoumarin, scopoletin, and rubiadin the electro-negative region is highly oriented around the ketone group (=O) and partially at another O atom in the pentagon. The compensating electropositive charge was distributed elsewhere. In aloe emodin, emodin, and curcumin the electronegativity was distributed around the ketone group while high electropositivity was observed around the substituted hydroxyl functional groups. In berberine electro negative region is very small and it is more electro-positive in nature. All the selected compounds have significantly greater dipole moment than standard urea (1.3732 Debye), specifically scopoletin and curcumin has 8 times greater value than urea. Concerning chemical potential, curcumin emerges as easily reactive, than berberine. The evaluation of NLO properties, including dipole moment (μ), polarizability (α), and mean first hyperpolarizability (β), underscores the superiority of berberine, making it highly reactive and easily activated during laser light irradiation.
Discussion and conclusion: Berberine exhibits superior NLO properties, marked by high reactivity, substantial softness, and significant first hyperpolarizability, making it the most effective photosensitizer among the studied phytochemicals for enhancing PDT efficacy in cancer treatments.

Introduction

Photodynamic therapy (PDT) stands is an innovative, clinically validated, and minimally invasive therapeutic approach for cancer treatment [1]. PDT is mostly utilized for actinic keratoses, superficial basal cell carcinomas, *in situ* squamous cell carcinomas (Bowen disease),

---

* Corresponding authors.
E-mail addresses: safnahussain2@gmail.com (K.P. Safna Hussan), kmuralika@gmail.com (K. Muraleedharan).

https://doi.org/10.1016/j.rechem.2024.101580
Received 27 May 2024; Accepted 3 June 2024

and superficial forms of skin cancer [2]. The concept of photodynamic therapy is that the photosensitizer, after being irradiated with light, particularly porfimer sodium (photofrin, which is a specific type of PDT agent) in the presence of oxygen become active to initiate a photochemical reaction that generates highly reactive oxygen species (ROS) such as hydroxyl radical ($OH^{\cdot}$), singlet oxygen ($^1O_2$), and super- oxide radical ($O_2^{\cdot -}$), leading to substantial cellular toxicity and ensuing cell death [1].

The effectiveness of photodynamic treatment (PDT) is dependent upon the selection of a photosensitizer which is a non-toxic active chemical substance. Based on the chemical structures of PS, it can be categorized into three distinct groups, porphyrin-based (photofrin), chlorophyll-based (chlorine), and dye (phthalocyanine). Most of the FDA-approved PS, that are being used in clinical studies belong to porphyrin-based [3]. Ideal photosensitizers (PS) for anticancer therapy must exhibit high red-range absorption (600–800 nm), efficiently transforming light into chemical energy upon encountering singlet oxygen or superoxide. The PS should be a single, non-toxic molecule with stability, low production cost, and tumor selectivity. Three generations, from porphyrins to modified compounds with biological couples, enhance therapeutic efficacy. Tetrapyrrole-based PS like phthalocyanines, bacteriochlorins, and chlorine, with deep-red absorption, improve tumor control by penetrating tissues more effectively [4].

Natural photosensitizers derived from plants, algae, and microorganisms have garnered significant attention in the field of photodynamic therapy. These substances exhibit superior photostability, heightened biocompatibility, improved bioavailability, and easier metabolism compared to some synthetic counterparts. Additionally, they demonstrate lower toxicity with specificity for certain cells. The abundant availability and cost-effectiveness of these natural photosensitizers have propelled their utilization in advanced therapeutic methods. Natural photosensitizers remain active and effective throughout light exposure during photodynamic therapy by absorbing higher energy in the UV region, including the Soret band in the blue region, and capable of raising molecules to higher energetic states, akin to red light easily [5]. Several natural compounds have been investigated as potential photosensitizers for photodynamic therapy (PDT) including chlorophyll and derivatives, hypericin, curcumin, phthalocyanines from spirulina, hypericin from algae, rose bengal, porphyrins from bacteria, hypericin from Chinese herb, anthocyanins, etc. Determining the chemical composition, natural sources, and phytopharmaceutical characteristics of natural photosensitizers may lead to the discovery of effective PDT alternatives found in nature. Research is ongoing to further understand and optimize the use of natural photosensitizers in photodynamic therapy and related fields.

Sulaiman et al. [1] recently explored the possibilities of photodynamic therapy (PDT) using herbal medicines. By revealing the tripartite components of PDT—photosensitizers, molecular oxygen, and light—and delineating the mechanism of tumor cell death through reactive oxygen species generation, those work underscore the pivotal role of photosensitizing agents in this therapeutic paradigm. Importantly, it draw attention to the underexplored realm of herbal medicines, rich in diverse phytochemical compounds with inherent photosensitizing properties, which served as a cornerstone for our work [5]. In that paper, a polyherbal formulation is used as photosensitizer in photodynamic therapy, in which the formulation compost of aloe vera, berberis aristata, curcuma longa, ficus religiosa, ipomoea mauritian and rubia cordifolia. From the LCMS reports they have concluded that the phytochemicals responsible for the photosensitizing action are aloe emodin, emodin, berberine, curcumin, furanocoumarin, scopoletin and rubiadin.

This paper embarks on a comprehensive analysis of the non-linear optical properties of phytochemical photosensitizers tailored for cancer PDT through quantum computational approaches, building upon the pioneering work of Sulaiman et al. Through a quantum mechanical approach, this work evaluate the non-linear optical properties of screened phytochemicals of the reported poly-herbal formulation from LCMS, including aloe emodin, emodin, berberine, curcumin, furanocoumarin, scopoletin, and rubiadin. By delving into their electronic structure and excited-state dynamics, this work elucidate the underlying mechanisms governing their photodynamic behavior. Additionally, we seek to discern the chemical behavioral changes of individual phytochemical compounds upon light irradiation, echoing the objectives outlined by Sulaiman et al by elucidating structural geometry, frontier molecular orbitals, and non-linear optical properties by quantum computational calculations performed at the DFT/B3LYP/6-311G+(d,p) level of theory. This study calculates the electric dipole moment (μ), polarizability (α), hyperpolarizability (β), and electrophilicity index (ω) values of selected phytochemical photosensitizers using DFT. These parameters are crucial for understanding the non-linear optical (NLO) properties and reactivity of these compounds in the context of photodynamic therapy (PDT). The dipole moment provides insights into the molecular polarity and its interaction with electric fields, polarizability reflects the molecule's ability to respond to external electric fields, influencing its optical refractive properties, hyperpolarizability is key to second-order NLO effects, such as second-harmonic generation, which are vital for photonic devices and the electrophilicity index helps assess the molecule's tendency to accept electrons, crucial for generating reactive oxygen species (ROS) in PDT. By integrating these computational studies, we aim to enhance the understanding of the electronic properties and reactivity of phytochemical photosensitizers in the herbal medicine, thereby facilitating their optimization for improved therapeutic outcomes in PDT. This approach underscores the importance of a theoretical foundation in advancing the application of herbal medicines in cancer treatment. Moreover, this interdisciplinary endeavor at the nexus of quantum chemistry, photophysics, and cancer therapeutics seeks to not only deepen our understanding of these phytochemical photosensitizers but also to facilitate the rational design of next-generation photosensitizers with enhanced phototoxicity and tumor-targeting capabilities, thus contributing to the ongoing advancements in PDT from theoretical predictions to experimental fruition.

Materials and methods

Materials

The photosensitizing compounds from *Aloe vera*, *Berberis aristata*, *Curcuma longa*, *Ficus religiosa*, *Ipomoea mauritiana*, *Rubia cordifolia* and the input structures these compounds were taken from the PubChem database. Their IDs as well as other details including medicinal properties were tabulated in Table 1 and chemical structures were depicted Fig. 1. The downloaded structures were in SDF (Standard Data File) format and converted to Gaussian input files using Open Babel Software.

Computational details

All the quantum calculations have been performed by density functional theory using a Gaussian09 software package. The initial geometry chosen for calculation was taken from the PubChem database and optimized with the B3LYP/6–311++G (d, p) level of the theory [14,15]. The optimized geometry was compared to crystallographic data [16] in the Phytochemistry Division, Center of Medicinal Plants Research, Arya Vaidya Sala Kotakkal such comparison between the experimental and theoretical values helps to reduce the error in the optimized geometry. The optimized geometry was used for the calculations of bond length, bond angle, and energy at the B3LYP/6-311++ G (d,p) method. The non–linear optical property analysis of the compounds was done at B3LYP/6-311++G (d, p) level within the Gaussian 09 package program (Frisch et al., 1998) [17]. Dipole moments, polarizability, and hyper polarizability were also calculated at the same level of theory. See (Fig. 2).

Table 1
The details of selected phytochemicals compounds:

Phytochemicals	PubChem ID	Source Plant	Absorption Wavelength (nm)	Medicinal Properties	References
Aloe-emodin	10,207	Aloe vera	370 to 500	anticancer, antivirus, anti-inflammatory, antibacterial, antiparasitic, neuroprotective, and hepatoprotective	[67]
Emodin	3220	Aloe vera	370 to 500	anticancer, anti-inflammatory, antioxidant, antibacterial, antivirus, anti-diabetes	[8]
Berberine	2353	Berberis aristatn	250 to 350	immunomodulatory, antioxidative, cardioprotective, hepatoprotective, and renoprotective	[9]
Curcumin	969516	Curcuma longa	350 to 450	antioxidant, anti-inflammatory, neuroprotective, anticancer, hepatoprotective, and cardioprotective	[10]
Furanocoumarin	68082	Ficus religiosa	320 to 380	antioxidants, antibacterial, analgesic, anticonvulsive, anticoagulant, hypotensive, antidepressants, antifungal, antiviral, anti-inflammatory, antiallergic	[11]
Scopoletin	5280460	Ipomoea mauritiana	250 to 350	antibacterial, antifungal, anti-inflammatory	[12]
Rubiadin	124062	Rubin cordifolia	350 to 450	anticancer, antiosteoporotic, hepatoprotective, antiepileptic, neuroprotective, anti-inflammatory, antidiabetic, antioxidant, antibacterial, antimalarial, antifungal, and antiviral	[13]

Source plant, PubChem ID, and their medicinal properties [5].

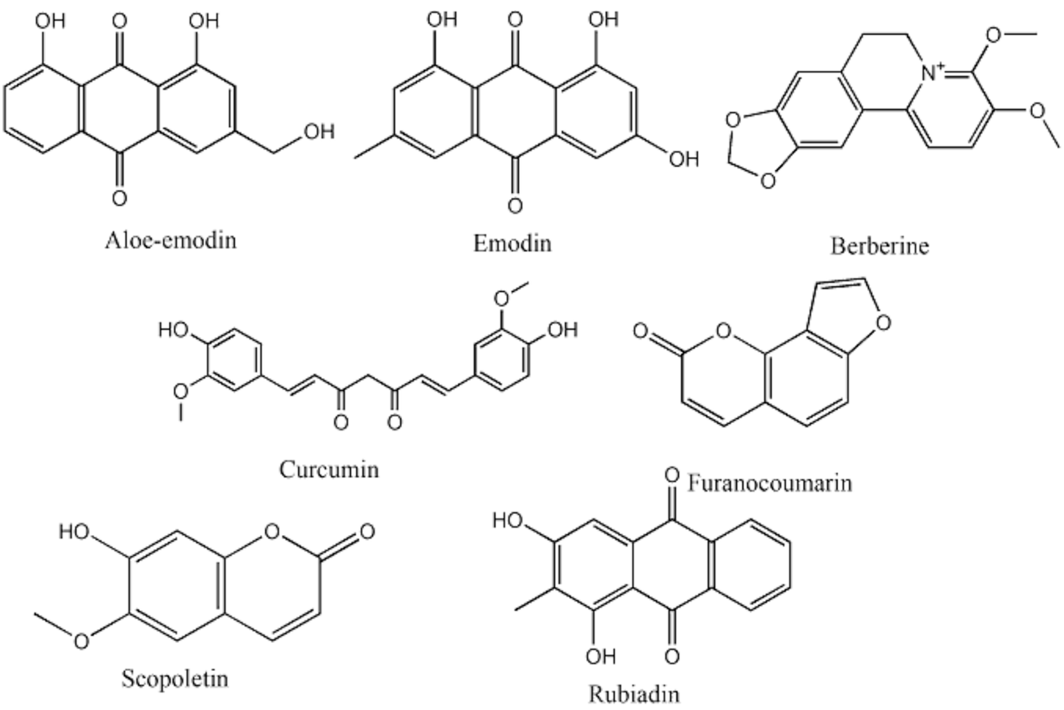

Fig. 1. Chemical Structure of selected chemical compounds from the reported polyhedral formulation with photosensitizing potential.

Results and discussions

The photo-sensitizing characteristics of these compounds, which are isolated from various medicinal plants, are explained in the paper "Photoactive Herbal Compounds: A Green Approach to Photodynamic Therapy," which was published by the Phytochemistry Division, Centre of Medicinal Plants Research, Arya Vaidya Sala Kottakkal. As natural photosensitizers in photodynamic treatment, they have employed a polyherbal mixture made from *Aloe vera, Berberis aristata, Curcuma longa, Ficus religiosa, Ipomoea Mauritian, and Rubia cordifolia*. Furthermore, Sulaiman et al. discovered that the most likely active phytochemical substances are in charge of producing reactive oxygen during photodynamic treatment when a laser is present. Gaining a thorough understanding of how each phytochemical molecule changes chemically and behaviorally in response to light radiation is the primary goal of this effort. To achieve that, an analysis of each compound's non-linear optical characteristics using a quantum mechanical technique has been conducted in order to identify the functional group in charge of the activity. The phytochemicals that have been chosen include scopoletin, berberine, curcumin, aloe emodin, emodin, and rubiadin.

Molecular geometry

Frontier molecular orbitals

In the context of photosensitizers, the Highest Occupied Molecular Orbital (HOMO) and the Lowest Unoccupied Molecular Orbital (LUMO) play crucial roles in the absorption and transfer of light energy and is often used to generate reactive oxygen species (ROS). When a photosensitizer absorbs a photon, an electron is promoted from the HOMO to the LUMO, creating an excited state. The energy difference between the HOMO and LUMO levels is critical in determining the efficiency of this excitation process and the energy stored in the HOMO-LUMO transition can be harnessed to produce highly reactive oxygen species, such as singlet oxygen, which can induce cellular damage and lead to the death of targeted cells. The isosurfaces of the outermost molecular orbital, where charge density is confined, are seen in Fig. 3. Furanocoumarin

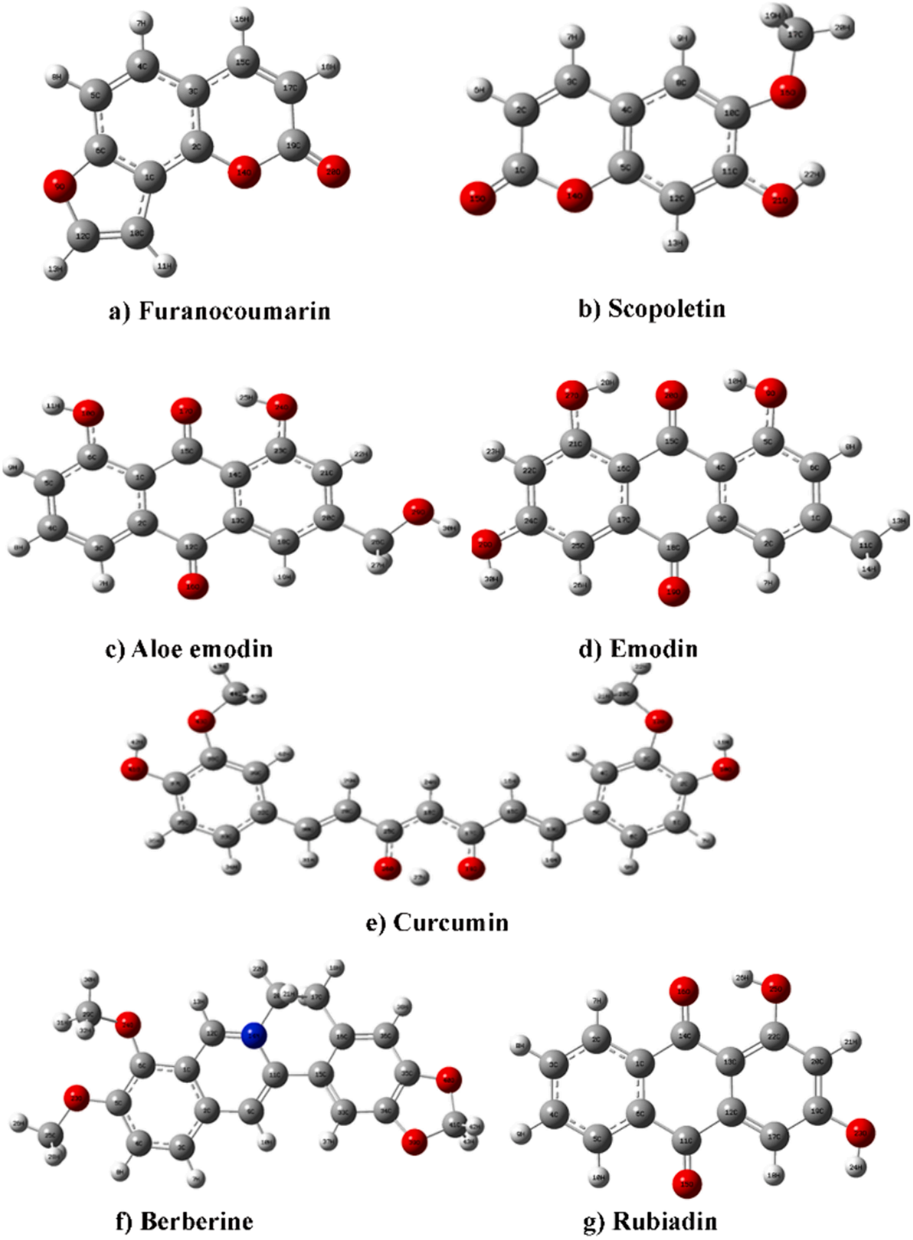

a) Furanocoumarin
b) Scopoletin
c) Aloe emodin
d) Emodin
e) Curcumin
f) Berberine
g) Rubiadin

Fig. 2. Optimized geometry at DFT/B3LYP/6-311++ G (d,p) method of active compounds in the reported polyhedral formulation with photosensitizing potential a) furanocoumarin, b) scolpoletin, c)aloe emodin, d) emodin, e) curcumin, f) berberine, g) rubiadin.

and scopoletin exhibit π-π* type electronic transitions upon exposure to UV radiation, whereas aloe-emodin, emodin, and rubiadin exhibit π-π type transitions. The π-s type is curcumin, while the π- σ * type is berberine. Understanding these distinctions is essential in elucidating the electronic behaviors of these compounds under UV radiation. The bandgap of aloe emodin, emodin curcumin, scopoletin berberine, furanocoumarin, rubiadin are 3.279 eV, 3.395 eV, 3.247 eV, 3.930 eV, 2.878 eV, 4.463 eV and 3.546 eV respectively. These distinctions in electronic transitions provide valuable insights into the molecular dynamics and photochemical behaviors of these compounds. The electronic transitions within a material influence its polarizability, resonant enhancement, hyperpolarizability, and symmetry properties, all of which are critical factors in determining the nonlinear optical properties of the material. These findings contribute to a deeper understanding of the non-linear optical properties of these compounds, paving the way for applications in photodynamic therapy. Since electronic transitions influence the material's ability to generate higher-order optical effects, such as second harmonic generation (SHG) and other nonlinear processes.

Molecular electrostatic potential map (MEP)

Electrostatic potential maps provide a visual representation of the charge distribution within a photosensitizer molecule, offering valuable information about its electronic structure, reactivity, and potential interactions with other molecules. This knowledge is essential for the rational design and optimization of photosensitizers with a deep understanding of electron donation and acceptance during photoexcitation.The electrophilic and nucleophilic sites in a molecule can easily be identified with the help of a molecular electrostatic potential map (MEP) which in turn determines the chemical reactivity of a compound that is responsible for non-covalent interactions [18]. For this reason, the MEP has been calculated for all the selected phytochemical compounds at the DFT/B3LYP/6311 G ++ (d, p). The ascending order of potential at the surface is represented by different colors, red < orange < yellow <

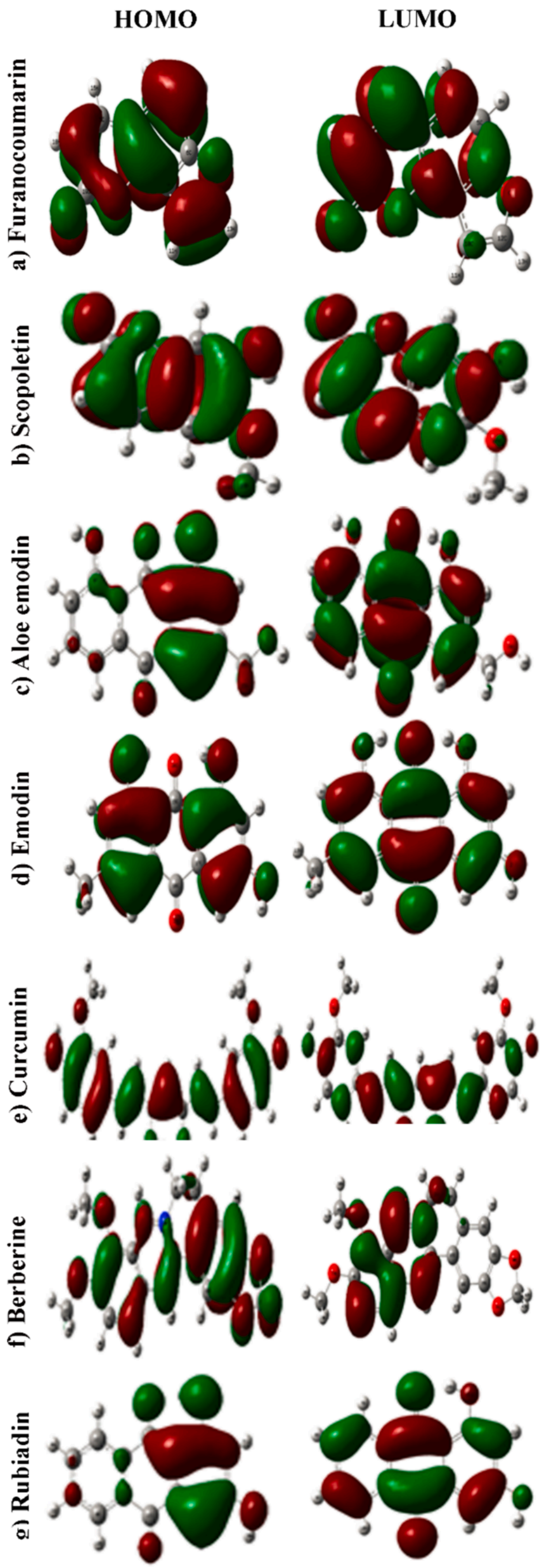

Fig. 3. The frontier molecular orbitals of optimized phytochemicals with DFT/B3LYP/6311 G ++ (d,p) a) furanocoumarin, b) scolpoletin, c)aloe emodin, d) emodin, e) curcumin, f) berberine, g) rubiadin. The distinct colors highlights electron density distributions.

green < blue. Red represents regions of most negative electrostatic potential, blue represents regions of most positive electrostatic potential and green represents regions of zero potential [19]. In the MEP map of furanocoumarin, scopoletin, and rubiadin the electro-negative region is highly oriented around the ketone group (C=O) and partially at another O atom in the pentagon. The compensating electropositive charge was distributed elsewhere. In aloe emodin, emodin, and curcumin the electronegativity was distributed around the ketone group while high electropositivity was observed around the substituted hydroxyl functional groups. In berberine electro negative region is very and it is more electro-positive. MEP maps show the possible sites for nucleophilic attack and electrophilic attacks. Fig. 4 shows the MEP of optimized phytochemical compounds.

Global descriptive parameters

Global descriptive parameters are key metrics that provide an overall characterization of the properties of molecules, and they play a crucial role in understanding and designing effective photosensitizers. These parameters offer a simplified and comprehensive view of a photosensitizer's behavior, allowing researchers to make informed decisions regarding its potential applications. According to Koopmans' theorem [20], through equations (E_{LUMO}), (E_{HOMO}), the HOMO and LUMO orbital energies are related to gas phase vertical ionization energies (I) and vertical electron affinities (EA) of the isomers. Electron affinity indicates the potential of a compound to accept precisely one electron from a donor. By using HOMO and LUMO energy values, global descriptors are calculated as follows.

$$\textit{Ionization potential}(IP) \approx -E_{HOMO}$$

$$\textit{Electron affinity}\ (EA) \approx -E_{LUMO}$$

where E_{HOMO} is the energy of HOMO and E_{LUMO} is the energy of LUMO.

$$\text{Hardness}\ (\eta) \approx \frac{IP - EA}{2}$$

$$\text{electronegativity}\ (\chi) \approx \frac{IP + EA}{2}$$

$$\text{Softness}\ (S) \approx \frac{1}{2\eta}$$

$$\textit{Chemical potential}\ (\mu) \approx -\chi$$

$$\text{Electrophilicity index}\ (\omega) \approx \frac{\mu^2}{2\eta}$$

Calculated global descriptors are tabulated in Table 2. Physically, chemical potential m describes the escaping tendency of electrons from an equilibrium system electrophilicity index is a measure of the stabilization in energy after a system accepts an additional amount of electronic charge from the environment. When two molecules react, which one will act as an electrophile (nucleophile) will depend upon the higher (lower) value of the electrophilicity index. The energy gap of all studied molecules are low indicating that they can absorb light at longer wavelengths, making it suitable for applications where visible or near-infrared light is prevalent. Among studied molecules berberine has the lowest HOMO-LUMO gap. The result emphasizes that the most reactive compound is berberine with high softness and low hardness value. The electron affinity of a photosensitizer reflects its tendency to accept electrons [21]. In that sense berberine is the best with higher electron affinity suggests a greater likelihood of accepting electrons during redox processes. At the same time, curcumin will easily donate one electron since it has low ionization potential, implies it can easily undergo charge transfer reactions during photoexcitation. while furanocoumarin will easily accept one electron since it has the lowest electron affinity.

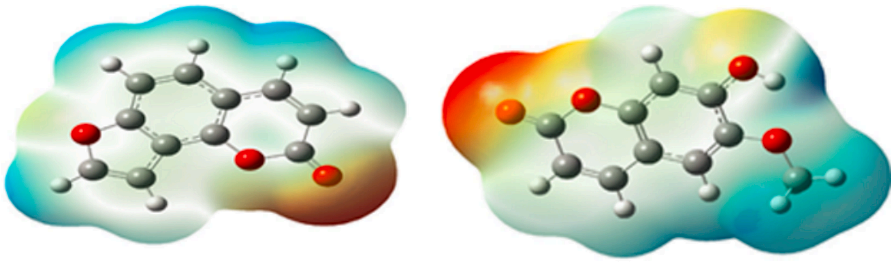

a) Furanocoumarin b) Scopoletin

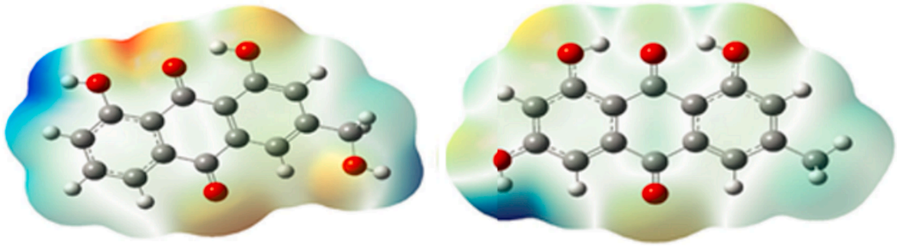

c) Aloe emodin d) Emodin

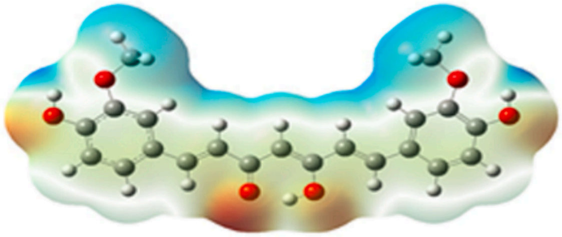

e) Curcumin

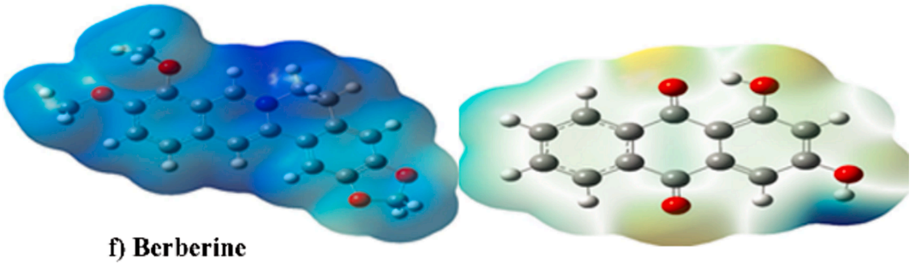

f) Berberine g) Rubiadin

Fig. 4. The MESP of optimized phytochemical compounds with DFT/B3LYP/6311 G ++ (d,p) a) furanocoumarin, b) scolpoletin, c)aloe emodin, d) emodin, e) curcumin, f) berberine, g) rubiadin. Colors indicate the electrostatic potential of a molecule's electron density, red signifies regions of high electron density, often indicating electron-rich or nucleophilic areas, while, blue represents regions of low electron density, suggesting electron-poor or electrophilic regions. (For interpretation of the references to colour in this figure legend, the reader is referred to the web version of this article.)

Table 2

The global descriptive parameters of optimized phytochemical compounds with DFT/B3LYP/6311 G ++ (d,p).

Slno	a	b	c	d	e	f	g
Molecule	**Aloe Emodin**	**Emodin**	**Furanocoumarin**	**Rubiadin**	**Scopoletin**	**Curcumin**	**Berberine**
Homo	−6.555	−6.583	−6.414	−6.688	−6.530	−5.556	−8.485
Lumo	−3.275	−3.188	−1.951	−3.142	−2.599	−2.308	−5.607
Bandgap	3.279	3.395	4.463	3.546	3.930	3.247	2.878
Ionization energy	6.555	6.583	6.414	6.688	6.530	5.556	8.485
Electron affinity	3.275	3.188	1.951	3.142	2.599	2.308	5.607
Hardness	1.639	1.697	2.231	1.773	1.965	1.623	1.439
Softness	0.304	0.294	0.224	0.281	0.254	0.307	0.347
Chemical potential	−4.915	−4.885	−4.182	−4.915	−4.564	−3.932	−7.046
Electrophilic index	7.367	7.030	3.919	6.812	5.302	4.762	17.250

Regarding chemical potential, curcumin will be easily reactive while berberine is less chemically reactive.

A correlation was observed between the LUMO (Lowest Unoccupied Molecular Orbital) energy levels and the electrophilicity index of the compounds. Fig. 5 illustrates the linear relationship between ω and the energy of LUMO with the correlation coefficient of 0.9964. This indicates that the ability of the LUMO to accept electrons determines the observed reactivity of the compounds. Compounds with lower LUMO energies tend to have higher electrophilicity indices, indicating a greater tendency to accept electrons. This relationship is particularly evident in berberine, which has a low LUMO energy and a high electrophilicity index, confirming its status as a highly reactive electrophile. Conversely, compounds with higher LUMO energies exhibit lower electrophilicity indices, suggesting a reduced ability to accept electrons. This trend aligns with the observed electronic properties of curcumin and furanocoumarin, which have distinct electron-donating and accepting behaviors, respectively [22–25].

Nonlinear optical property (NLO)

Nonlinear optical (NLO) properties refer to the response of a material to an intense electromagnetic field, particularly in the context of nonlinear optical processes. The interaction of photosensitizers with light is fundamental to their function, and their nonlinear optical properties can play a role in various applications. The NLO properties of these photosensitizers contribute to their effectiveness in PDT in several ways like two-photon absorption (TPA), enhanced imaging for targeting, tissue penetration and depth, enhanced selectivity, controlled generation of reactive oxygen species (ROS), combination with nonlinear optical imaging techniques, tailoring photosensitizer properties etc.

Organic molecules containing conjugated p electrons are characterized by large values of molecular first-order hyper-polarizability as analyzed using vibrational spectroscopy. They can manipulate photonic signals which are important for nonlinear optics. Materials possessing nonlinear optical properties (NLO) change the propagation characteristics (phase, frequency, amplitude, polarization, etc.) of the incident light. For a material to generate a second-order nonlinear optical effect, it should possess a non-centrosymmetric structure along the direction of the electric field. Only a material having a non-centrosymmetric structure will generate a nonlinear optical response. It indicates χ^2 is zero for centrosymmetric media. According to the classical theory of the Raman effect, when a molecule is placed in a static electric field, positively charged nuclei are attracted by the negative pole of the field and negatively charged electrons are attracted by the positive pole of the field. This separation of charges causes an induced dipole moment in the molecule and the molecule is said to be polarized. The induced dipole moment per unit volume is called polarization, P.

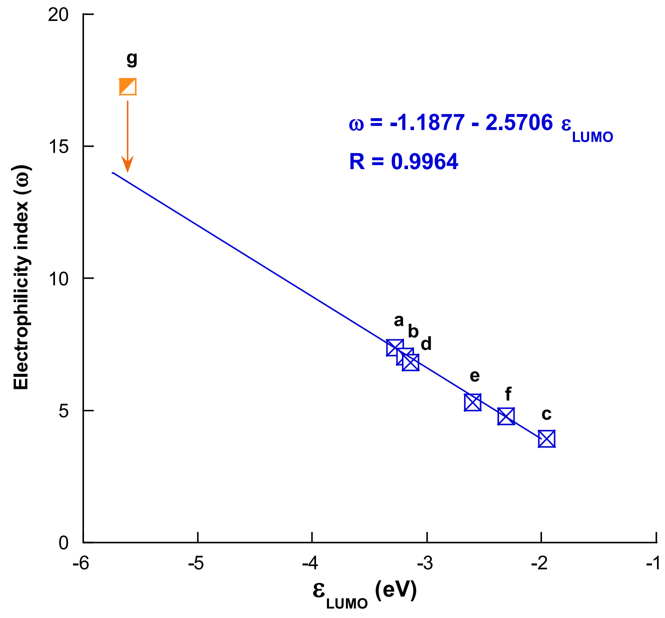

Fig. 5. Correlation between electrophilicity index (ω) calculated at B3LYP/6311 G++ (d,p) level for the compounds **a-g** listed in Table 2 and their LUMO orbital energy (ε_{LUMO}).

$$P = \chi eE$$

where χe is the linear susceptibility of a collection of molecules.

When a large electric field is incident upon an anisotropic material, the polarization may be expanded in a Taylor series to obtain

$$P = P_0 + \chi^{(1)}E + \chi^{(2)}E^2 + \chi^{(3)}E^3 + \dots\dots\dots\dots\dots$$

where $\chi^{(n)}$ is the nth-order susceptibility tensor of the bulk medium and E is the strength of the electric field. $\chi^{(1)}$ is alpha(α) and $\chi^{(2)}$ is hyperpolarizability(β).

In order to explore NLO properties of the title compound, the total static dipole moment μ, the linear polarizability β, the anisotropy of polarizability Δ α and the mean first-order hyper- polarizability β are calculated from the optimized structures of the phytochemicals using the B3LYP/6311 G ++ (d, p) level of theory. All the calculations of the molecules were done in the gas phase of the compound based on the finite-field approach. The first-order hyperpolarizability is a third-rank tensor that can be described by a 3 × 3 × 3 matrix. The 27 components of the 3D matrix can be reduced to 10 components due to Kleinman symmetry. It can be given in the lower tetrahedral format. The lower part of the 3 × 3 × 3 matrices is tetrahedral. The components β are the coefficients in the Taylor series expansion of the energy in the external electric field.

The dipole moment is a measure of the separation of positive and negative charges within a molecule, and it can influence various aspects of the photosensitizer's behavior during the PDT process. The dipole moment, for instance, affects the photosensitizer's molecular orientation in the cellular environment, including biomolecules in the target cells, which affects the PDT process's effectiveness. More over, it can impact the interaction of the photosensitizer with cellular components, such as membranes and proteins and influence how the photosensitizer aligns in response to these external fields, affecting the overall effectiveness of the treatment. The dipole moment of a molecule interacting with an electric field can be written as,

$$\mu_i = \mu_i^0 + \alpha_{ij}F_j + (1/2)\beta_{ijk}F_jF_k + (1/6)\Upsilon_{ijkl}F_jF_kF_l + \dots\dots\dots\dots\dots\dots$$

where μ_i^0 is the permanent dipole moment and α_{ij}, β_{ijk}, $\Upsilon_{ijk}$are tensor elements of the linear polarizability and first and second hyperpolarizabilities respectively. The second-order term of hyper polarizability gives rise to sum and difference frequency mixing (including second harmonic generation) and optical rectification. The third-order term is responsible for the third harmonic generation and two-photon resonances. From our DFT calculations, the total dipole moments (μ) of the studied compounds range from 1.444 D to 8.660 D, which are significantly greater dipole moment than standard urea (1.3732 D). The individual components of the dipole moment vector (μx, μy, μz) and their total values for aloe emodin, emodin, ffuranocoumarin, rrubiadin, sscopoletin, ccurcumin, and bberberine are provided in Table 3. It is noteworthy that for all studied compounds, the dipole moment in the z direction is negligible, indicating that the polarity is primarily confined to the x and y directions. The significant dipole moments in the ground state (μ_G) suggest substantial charge transfer from the electron-donating groups, enhancing their effectiveness as photosensitizers in PDT. These results underscore the importance of dipole moments in determining the efficiency of these compounds as photosensitizers, with Scopoletin and Curcumin standing out due to their exceptionally high dipole moments, indicating superior potential for photodynamic therapy applications [23].

Table 3

The dipole moment of optimized phytochemical compounds with DFT/B3LYP/6311 G ++ (d,p).

Molecule	Dipole Moment			
	μ_x	μ_y	μ_z	Total Dipole moment (Debye)
a. AloeEmodin	−1.061	−0.812	−0.5493	1.444
b. Emodin	−1.4843	−2.966	0.0003	3.316
c. Furanocoumarin	−2.4548	3.552	−0.0011	4.317
d. Rubiadin	−2.2207	−2.062	−0.0004	3.030
e. Scopoletin	6.6446	−5.555	−0.0015	8.660
f. Curcumin	0.3282	8.339	−0.0007	8.345
g. Berberine	−3.4257	0.6489	0.5573	3.530

Polarizability plays a significant role in the design and effectiveness of photosensitizers used in PDT, since it has influence on the molecule's electronic structure, interactions with light, and its ability to generate reactive oxygen species (ROS) upon light activation. Photosensitizers with higher polarizability may have enhanced absorption of light in the visible and near-infrared regions, it can impact the molecule's light-harvesting efficiency, ensuring that a higher percentage of absorbed photons leads to the generation of excited states and subsequently reactive oxygen species and to generate singlet oxygen ($^1O_2$) through energy transfer mechanisms upon light activation, which are crucial for effective penetration into tissues during PDT. Moreover, the polarizability of a photosensitizer may also influence its biocompatibility and pharmacokinetic properties. A well-designed photosensitizer with appropriate polarizability is more likely to exhibit favorable distribution, retention, and elimination characteristics within the body. Thus, measuring the polarizability are essential to analyse materials' NLO to determine the photosensitizing behavior of phytochemicals. The polarizability and hyperpolarizability of NLO can be written as tensors. While the linear polarizability tens α as shown below is a 3*3 matrix having 9 components, $\begin{bmatrix} \alpha_{xx} & \alpha_{xy} & \alpha_{xz} \\ \alpha_{yx} & \alpha_{yy} & \alpha_{yz} \\ \alpha_{zx} & \alpha_{zy} & \alpha_{zx} \end{bmatrix}$,

$$\alpha_{total=}\frac{(\alpha_{xx} + \alpha_{yy} + \alpha_{zz})}{3}$$

and anisotropy of polarizability

$$\Delta\alpha = \frac{1}{\sqrt{2}}\sqrt{[(\alpha_{XX} - \alpha_{YY})^2 + (\alpha_{YY} - \alpha_{ZZ})^2 + (\alpha_{ZZ} - \alpha_{XX})^2 + 6\alpha_{XZ}{}^2]}$$

The polarizability and anisotropy of polarizability of all selected samples were calculated in atomic units (a.u.) and then converted to Å^3, (1a.u is 0.1482 × 10^{-24} Å^3 for β) and tabulated in Table 4. All the selected compounds have higher polarizability values compared to urea. Furanocoumarin, scopoletin and berberine have the higher values in comparison [26–29]

It's important to note that while hyperpolarizability can be a relevant property, the primary mechanisms for PDT effectiveness usually involve one-photon absorption, singlet oxygen generation, and subsequent cellular damage. The consideration of hyperpolarizability is often more specialized and may be explored in conjunction with advanced optical techniques or in situations where nonlinear optical processes can be advantageous. For the first hyper polarizability, the quantity of interest is given by

$$\beta_{total} = \left[(\beta_{xxx} + \beta_{xyy} + \beta_{xzz})^2 + \left(\beta_{yyy} + \beta_{yzz} + \beta_{yxx}\right)^2 + \left(\beta_{zzz} + \beta_{zxx} + \beta_{zyy}\right)^2 \right]^{1/2}$$

For a material to have strong second-order NLO properties, one of the requirements is that the material should have a large molecular hyperpolarizability (β). Since the existence of large molecular hyperpolarizability is the basis of strong Second Harmonic Generation (SHG), organic molecules with long conjugation systems that usually exhibit large β values are certainly candidate molecules for NLO materials. The large value of the first hyperpolarizability, β, is associated with the intramolecular charge transfer resulting from an electron cloud movement through a π conjugated framework from electron donor to electron acceptor groups. With an increase in conjugation length between the donor and the acceptor, the magnitudes of molecular polarizability and hyperpolarizability coefficients are found to increase superlinearly. The hyperpolarizability values of selected phytochemicals were calculated in e.s.u and converted to a.u (1 a.u is 0.0086393 10^{-30} for β) and tabulated in Table 5. The first order hyperpolarizability of all phytochemicals are significantly greater than that of Urea value (0.3728 × 10^{-30}) > 100 times. These results confirm that all the selected phytochemicals have good nonlinear optical property and can be best candidate for photosensitizers in PDT. Scopoletin and berberine is easily reactive, among them berberine have the best nonlinear optical properties and can be easily activate during irradiation with laser light when compared to others [27].

Conclusion

Upon analyzing the structural and electronic properties, including frontier molecular orbitals (HOMO, LUMO), bond dissociation energy (BDE), ionization potential (IP), electron affinity (EA), softness (η), hardness (S), as well as parameters like pi (π) and chi (ξ), through quantum mechanical calculations at the B3LYP/6-311G++(d,p) level of theory, all the phytochemical compounds emerged as promising candidates for photosensitizers. However, berberine stood out as the most reactive compound, displaying high softness and low hardness, indicative of its heightened chemical reactivity. Curcumin demonstrated a propensity to donate electrons, while furanocoumarin showed a tendency to accept electrons. The study also explored nonlinear optical (NLO) properties, revealing that scopoletin and berberine surpassed urea as benchmarks in this regard. Notably, berberine exhibited superior nonlinear optical properties, suggesting heightened responsiveness during laser light irradiation. Scopoletin and Curcumin presented in these work exhibit high dipole moments, indicating their suitability for NLO applications due to their high dipole moments. The strong polarization characteristics within these molecules suggests that they possess

Table 4

The polarizability, α in 10^{-24} esu of optimized phytochemical compounds, a) aloeemodin, b) emodin, c) furanocoumarin, d) rubiadin, e) scopoletin, f) curcumin, g) berberine with DFT/B3LYP/6311 G ++ (d,p).

Sl no	α_{xx}	α_{yy}	α_{zz}	α_{xy}	α_{xz}	α_{yz}	α_{total}	$(\alpha_{xx}-\alpha_{yy})^2$	$(\alpha_{yy}-\alpha_{zz})^2$	$(\alpha_{zz}-\alpha_{xx})^2$	Δα	Δα(a.u)
a)	−58.14	−132.05	−117.09	2.82	−3.047	0.870	−102.43	5462.99	223.78	3475.42	68.08	10.08
b)	−104.22	−121.65	−116.83	−4.00	−0.001	0.003	−114.23	303.85	23.18	159.16	17.06	2.52
c)	−84.47	−73.22	−82.35	16.81	−0.003	0.002	−80.01	126.55	83.37	4.49	30.91	4.58
d)	−87.90	−109.52	−105.24	−10.30	0.0030	0.003	−100.89	467.41	18.35	300.50	26.67	3.95
e)	−89.78	−75.80	−82.66	0.88	−0.002	−0.000	−82.75	195.43	47.07	50.68	12.20	1.80
f)	−178.9	−137.18	−166.30	−0.99	0.009	0.000	−160.81	1746.99	847.97	160.70	37.15	5.50
g)	−40.61	−108.60	−142.90	6.15	−2.436	2.889	−97.37	4622.62	1176.38	10462.89	91.03	13.49

significant charge separation and asymmetry, essential attributes for efficient response to external electric fields elucidates the nuanced electronic structure and charge distribution within these molecules, providing valuable information for their utilization in NLO materials and devices. These findings provide valuable insights into the potential application of these herbal compounds in photodynamic therapy. Berberine, with its exceptional reactivity and outstanding nonlinear optical properties, emerges as a promising candidate for further exploration in the development of effective and environmentally friendly photosensitizers for photodynamic therapy strategies.

Table 5
Hyperpolarizabilities of optimized compounds with DFT/B3LYP/6311 G ++ (d,p).

Molecule	β_{xxx}	β_{yyy}	β_{zzz}	β_{xzz}	β_{xyy}	β_{yxx}	β_{yzz}	β_{zxx}	β_{zyy}	$(\beta_{xxx} + \beta_{xzz} + \beta_{xyy})^2$	$(\beta_{yyy} + \beta_{yxx} + \beta_{yzz})^2$	$(\beta_{zzz} + \beta_{zxx} + \beta_{zyy})^2$	β_0(a.u) $\times 10^{-30}$
a) AloeEmodin	40.15	−6.37	0.21	7.03	−18.32	−18.4	6.44	−11.42	−0.632	833.37	336.08	140.19	313
b) Emodin	−73.3	−6.72	0.005	5.01	35.57	−80.07	3.84	0.005	0.003	1070.71	6881.01	0.0002	770
c)Furanocoumarin	−29.34	12.21	0.001	4.84	−32.99	24.18	−6.87	−0.01	−0.0001	3304.67	871.56	0.00008	558
d) Rubiadin	−78.24	−13.52	0.003	11.38	23.35	−39.86	1.81	−0.002	−0.006	1892.18	2660.04	0.00003	583
e) Scopoletin	184.96	−21.03	0.003	1.37	6.22	−54.61	4.77	−0.03	0.001	37079.19	5022.89	0.0006	1770
f) Curcumin	0.376	127.69	0.002	−0.22	4.86	145.92	12.28	−0.026	−0.009	25.13	81741.44	0.001	2470
g) Berberine	−123.66	23.44	3.727	−0.39	−34.98	−119.47	5.36	16.63	−2.12	25291.97	8217.839	332.26	1590

CRediT authorship contribution statement

V.M. Aneesa: Writing – original draft, Data curation, Formal analysis. **K.P. Safna Hussan:** Validation, Visualization, Writing – original draft, Data curation, Formal analysis, Methodology. **S. Lekshmi:** Writing – review & editing, Visualization, Formal analysis. **Thekkekara D. Babu:** Writing – review & editing, Supervision, Resources, Project administration, Funding acquisition. **K. Muraleedharan:** Writing – review & editing, Supervision.

Declaration of competing interest

The authors declare that they have no known competing financial interests or personal relationships that could have appeared to influence the work reported in this paper.

Acknowledgment

The authors thankfully acknowledge the Central Sophisticated Instrument Facility (CSIF) of the University of Calicut for providing Schrodinger Maestro software and hardware support.

References

[1] M. Lan, S. Zhao, W. Liu, C.S. Lee, W. Zhang, P. Wang, Photosensitizers for photodynamic therapy, Adv. Healthc. Mater. 8 (2019) 1–37, https://doi.org/10.1002/adhm.201900132.

[2] Photodynamic Therapy (PDT) for skin cancer, (n.d.). https://www.cancerresearchuk.org/about-cancer/skin-cancer/treatment/photodynamic-therapy#:~:text=for skin cancer-,Photodynamic Therapy (PDT) for skin cancer, skin cancer and surrounding area.

[3] M.G. Vicente, Porphyrin-based sensitizers in the detection and treatment of cancer: recent progress, Curr. Med. Chem. Anticancer. Agents. 1 (2001) 175–194, https://doi.org/10.2174/1568011013354769.

[4] P. Agostinis, K. Berg, K.A. Cengel, T.H. Foster, A.W. Girotti, S.O. Gollnick, S. M. Hahn, M.R. Hamblin, A. Juzeniene, D. Kessel, M. Korbelik, J. Moan, P. Mroz, D. Nowis, J. Piette, B.C. Wilson, J. Golab, Photodynamic therapy of cancer: an update, CA Cancer J. Clin. 61 (2011) 250–281, https://doi.org/10.3322/caac.20114.

[5] C. Sulaiman, B.P. George, I. Balachandran, H. Abrahamse, Photoactive herbal compounds: a green approach to photodynamic therapy, Molecules 27 (2022) 1–13, https://doi.org/10.3390/molecules27165084.

[6] B. Lv, K. Zheng, Y. Sun, L. Wu, L. Qiao, Z. Wu, Y. Zhao, Z. Zheng, Network pharmacology experiments show that emodin can exert a protective effect on MCAO rats by regulating Hif-1α/VEGF-a signaling, ACS Omega 7 (2022) 22577–22593, https://doi.org/10.1021/acsomega.2c01897.

[7] D. Xin, H. Li, S. Zhou, H. Zhong, W. Pu, Effects of anthraquinones on immune responses and inflammatory diseases, Molecules 27 (2022) 1–25, https://doi.org/10.3390/molecules27123831.

[8] M. Peng, Z. Zheng, S. Chen, L. Fang, R. Feng, L. Zhang, Q. Tang, X. Liu, Sensitization of non-small cell lung cancer cells to gefitinib and reversal of epithelial-mesenchymal transition by aloe-emodin via PI3K/Akt/TWIS1 signal blockage, Front. Oncol. 12 (2022) 1–9, https://doi.org/10.3389/fonc.2022.908031.

[9] W. Chang, K. Li, F. Guan, F. Yao, Y. Yu, M. Zhang, G.M. Hatch, L. Chen, Berberine pretreatment confers cardioprotection against ischemia-reperfusion injury in a rat model of type 2 diabetes, J. Cardiovasc. Pharmacol. Ther. 21 (2016) 486–494, https://doi.org/10.1177/1074248415627873.

[10] S.C. Gupta, S. Patchva, B.B. Aggarwal, Therapeutic roles of curcumin: lessons learned from clinical trials, AAPS J. 15 (2013) 195–218, https://doi.org/10.1208/s12248-012-9432-8.

[11] S. Ahmed, H. Khan, M. Aschner, H. Mirzae, E.K. Akkol, R. Capasso, Anticancer potential of furanocoumarins: mechanistic and therapeutic aspects, Int. J. Mol. Sci. 21 (2020) 1–20, https://doi.org/10.3390/ijms21165622.

[12] P. Kashyap, H. Ram, S.D. Shukla, S. Kumar, Scopoletin: antiamyloidogenic, anticholinesterase, and neuroprotective potential of a natural compound present in argyreia speciosa roots by in vitro and in silico study, Neurosci. Insights. 15 (2020), https://doi.org/10.1177/2633105520937693.

[13] Z. Peng, G. Fang, F. Peng, Z. Pan, Z. Su, W. Tian, D. Li, H. Hou, Effects of rubiadin isolated from prismatomeris connata on anti-hepatitis B virus activity in vitro, Phyther. Res. 31 (2017) 1962–1970, https://doi.org/10.1002/ptr.5945.

[14] E.E. Bolton, Y. Wang, P.A. Thiessen, S.H. Bryant, PubChem: integrated platform of small molecules and biological activities, in: Annu. Rep. Comput. Chem., 2008: pp. 217–241.

[15] K.P.S. Hussan, M.S. Thayyil, V.K. Rajan, K. Muraleedharan, DFT studies on global parameters, antioxidant mechanism and molecular docking of amlodipine besylate, Comput. Biol. Chem. 80 (2019) 46–53, https://doi.org/10.1016/j.compbiolchem.2019.03.006.

[16] J.C. Burley, Structure and intermolecular interactions of glipi- zide from laboratory X-ray powder diffraction research papers, Acta Crystallogr. Sect. B. B (2005) 710–716, https://doi.org/10.1107/S0108768105025991.

[17] M.J. Frisch, G.W. Trucks, H.B. Schlegel, G.E. Scuseria, M.A. Robb, C. J.R., G. Scalmani, V. Barone, B. Mennucci, G.A. Petersson, H. Nakatsuji, M. Caricato, X. Li, H.P. Hratchian, A.F. Izmaylov, J. Bloino, G. Zheng, J.L. Sonnenberg, M. Hada, M. Ehara, K. Toyota, R. Fukuda, J. Hasegawa, M. Ishida, T. Nakajima, Y. Honda, O. Kitao, H. Nakai, E. T. Vreven, J.A. Montgomery, Jr., J.E. Peralta, F. Ogliaro, M. Bearpark, J.J. Heyd, A. Brothers, K.N. Kudin, V.N. Staroverov, R. Kobayashi, J. Normand, K. Raghavachari, M.K. Rendell, J.C. Burant, S.S. Iyengar, J. Tomasi, M. Cossi, N. Rega, J.M. Millam, R.E.S. J.E. Knox, J.B. Cross, V. Bakken, C. Adamo, J. Jaramillo, R. Gomperts, K.M. O. Yazyev, A.J. Austin, R. Cammi, C. Pomelli, J. Ochterski, R.L. Martin, O. V.G. Zakrzewski, G.A. Voth, P. Salvador, J.J. Dannenberg, S. Dapprich, A.D. Daniels, D.F. Farkas, J.B. Foresman, J. V. Ortiz, J. Cioslowski, J., GAUSSIAN 09 (Revision A.2) Gaussian, Inc., Wallingford, CT, D. J. Gaussian 09,. B.01; (1998).

[18] B.S. Kusmariya, A.P. Mishra, Experimental, theoretical and docking studies of 2-hydroxy Schiff base type compounds derived from 2-amino-4-chlorobenzenethiol, J. Mol. Struct. 1101 (2015) 176–188, https://doi.org/10.1016/j.molstruc.2015.08.026.

[19] K.G. Sangeetha, K.K. Aravindakshan, K.P. Safna Hussan, Insight into the theoretical and experimental studies of 1-phenyl-3-methyl-4-benzoyl-5-pyrazolone N(4)-methyl-N(4)- phenylthiosemicarbazone - a potential NLO material, J. Mol. Struct. 1150 (2017), https://doi.org/10.1016/j.molstruc.2017.08.078.

[20] T. Koopmans, Über die zuordnung von wellenfunktionen und eigenwerten zu den einzelnen elektronen eines atoms, Physica 1 (1934) 104–113, https://doi.org/10.1016/S0031-8914(34)90011-2.

[21] H. Ji, L. Shen, Density Functional Theory Study of the Photosensitization Mechanisms of Indigo 7 (2009) 505–507, https://doi.org/10.2478/s11532-009-0044-9.

[22] Z.A. Guo, J.Y. Xian, L.R. Rong, H. Qin, Z. Jie, Theoretical study of metal ion impact on geometric and electronic properties of terbutaline compounds, Monatsh. Chem. 150 (2019) 1355–1364, https://doi.org/10.1007/s00706-019-02419-1.

[23] H. Raissi, I. Chérif, I. Aribi, H. Ayachi, A. Haj Said, S. Ayachi, T. Boubaker, Structure–property relationships in para-substituted nitrobenzofurazans: electrochemical, optical, and theoretical analysis, Chem. Pap. 76 (2022) 4059–4080, https://doi.org/10.1007/s11696-022-02150-y.

[24] W. Gabsi, T. Boubaker, R. Goumont, Azo-coupling reactions of para-X-benzenediazonium cations with 3-ethoxythiophene in acetonitrile, Int. J. Chem. Kinet. 48 (2016) 266–273, https://doi.org/10.1002/kin.20989.

[25] H. Raissi, H. Ayachi, F. Mahdhaoui, S. Ayachi, T. Boubaker, Relationships between experimental and theoretical scales of electrophilicity of 7-L-4-nitrobenzofurazans, J. Mol. Struct. 1224 (2021), https://doi.org/10.1016/j.molstruc.2020.128843.

[26] S.Z.S. El Behi, S. Ayachi, Computational modeling for the design of new fluorescent organic compounds based on both diketopyrrolopyrrole and nitrobenzofurazan moieties, J. Mol. Liq. 360 (2022).

[27] S.A. Balkis Abdelaziz, Z. Mazouz, B. Gassoumi, N. El Islam, S.P. Boukortt, Molecular engineering of D-π-A-type structures based on nitrobenzofurazan (NBD) derivatives for both organic solar cells and nonlinear optical response, J. Mol. Liq. 395 (2024).

[28] B. Abdelaziz, I. Ch, B. Gassoumi, S. Patane, S. Ayachi, Linear and nonlinear optical responses of nitrobenzofurazan- sulfide derivatives : DFT-QTAIM investigation on twisted intramolecular charge transfer, (2023). https://doi.org/10.1021/acs.jpca.3c04277.

[29] S.A. Imen Chérif, H. Raissi, K. Abiedh, B. Gassoumi, M.T. Caccamo, S. Magazu, A. H. Said, F. Hassen, T. Taoufik, Computational studies on optoelectronic and nonlinear optical properties of para-substituted nitrobenzofurazan compound, Mater. Today Commun. 35 (2023).